TRANSPORTATION RESEARCH

RECORD

JOURNAL OF THE TRANSPORTATION RESEARCH BOARD

NO.

1684

Issues in the Design of New and Rehabilitated Pavements

Pavement Design, Management, and Performance

A PEER-REVIEWED PUBLICATION OF THE TRANSPORTATION RESEARCH BOARD

TRANSPORTATION RESEARCH BOARD — NATIONAL RESEARCH COUNCIL

NATIONAL ACADEMY PRESS
Washington, D.C. 1999

Mechanistic Reappraisal of the Current Design Methodology for Rigid Airfield Pavements

YING-HAUR LEE

The current design methodology for rigid airfield pavements, based on the plate theory approach, was reevaluated in an attempt to accommodate the new Boeing B-777 airplanes. The differences between the conventional FAA design method and the newly developed Layered Elastic Design–FAA design methodology are investigated. The original concept of pass-to-coverage ratio is reevaluated. The prediction models developed are used for the estimation of critical edge stresses for design. The problems and difficulties of the conventional method, especially in the conversion of different aircraft types, are identified. The concept of cumulative damage factor should be used to account for the combined damages of different aircraft types and departures. Structural deterioration relationships are compared and tentative modification alternatives are explored. Consequently, the concept of an equivalent stress factor is introduced and an alternative structural deterioration model is proposed for trial design applications. Further investigations and verifications should be conducted as well.

Structural analysis of pavement systems has evolved from the classical solutions derived by Westergaard for rigid pavements and by Burmister for flexible pavements. Westergaard (*1*) idealized a concrete pavement as an infinite or semi-infinite elastic plate resting on a dense liquid (or Winkler) foundation with full contact between the slab-subgrade interface. Burmister (*2*) later developed closed-form solutions based on the idealization of a flexible pavement as a layered elastic system. The conventional FAA (*3*) thickness design methodology for rigid airfield pavements was based on the plate theory and Westergaard's analytical solution for edge loading conditions. When the main gear assembly is analyzed by using the conventional FAA design procedures, "the pavement thickness requirements are considered to be unduly conservative" (*4*), which is especially noticeable for flexible pavements on weak subgrades. Thus, FAA recently has issued a new advisory circular which uses "the multi-layered linear elastic theory" for the design of both flexible and rigid airfield pavements to accommodate the new Boeing B-777 airplanes (*4*). Computerized design procedures are coded in the Layered Elastic Design–FAA (LED–FAA) program. Nevertheless, the applicability of layered elastic theory in concrete pavement design has always been questioned and debated over the decades, which warrants the need for further investigations. Consequently, the main objective of this study was to reevaluate the current design methodology for rigid airfield pavements, particularly those based on the conventional plate theory approach (*5*).

Department of Civil Engineering, Tamkang University, E725, 151 Ying-Chuan Road, Tamsui, Taipei, Taiwan, Republic of China.

REEVALUATION OF PASS-TO-COVERAGE RATIO CONCEPT

The pass-to-coverage ratio concept was developed on the basis of the assumption that airfield traffic is normally distributed instead of uniformly distributed. As shown in Figure 1(*a*), the distribution curve represents the lateral placement frequency of the centerline of one wheel on the aircraft. This specific shape may be described by the wander width W_w, over which the centerline of the aircraft traffic is distributed 75 percent of the time (*6*). It was considered that coverage represents the maximum number of tire prints applied to the pavement surface at that point where maximum accumulation occurs. The effect of the edge of a tire at 0 is assumed as detrimental as the effect of the tire centerline at 0. Thus, the accumulations at 0 may be expressed by the following equation:

$$\text{Coverages} = \int_{-\frac{W_t}{2}}^{\frac{W_t}{2}} P_t(x)dx = (C_x)(W_t)$$

$$P_t(x) = \frac{1}{\sigma_x\sqrt{2\pi}} e^{-\frac{1}{2}\left(\frac{x-u}{\sigma_x}\right)^2}$$

$$\text{P C} = \frac{1}{(C_x)(W_t)} \tag{1}$$

where

$P_t(x)$ = frequency of aircraft centerline passes per unit width;
C_x = maximum ordinate on the normal distribution curve;
W_t = tire width;
x = lateral placement of wheel center line;
u = mean value of the normal distribution curve; and
σ_x = standard deviation of the normal distribution curve.

Thus, the reciprocal of coverage or $(C_t)(W_t)$ is referred to as the pass-to-coverage (P/C) ratio.

This method was also extended to aircraft having many wheels by graphical addition of any number of single-wheel traffic distribution curves. As the wheel spacing becomes smaller, as shown in Figure 1(*b*), the general normal distribution curve for each single-wheel overlap can be expressed by Equation 2. In this case, graphical addition of the individual single-wheel curves results in a cumulative distribution curve with a maximum ordinate (C_w) greater than that of either single-wheel curve (C_x). Thus, the coverage per one aircraft pass can be approximated by the value of $(C_w)(W_t)$ (*6,7*). For example, as the wheel spacing becomes smaller and smaller or even is set to the extreme ($s = W_t$), the general normal distribution curves for each single wheel will approximately overlap each other. This special case is analogous to a single wheel load with doubled weight and doubled

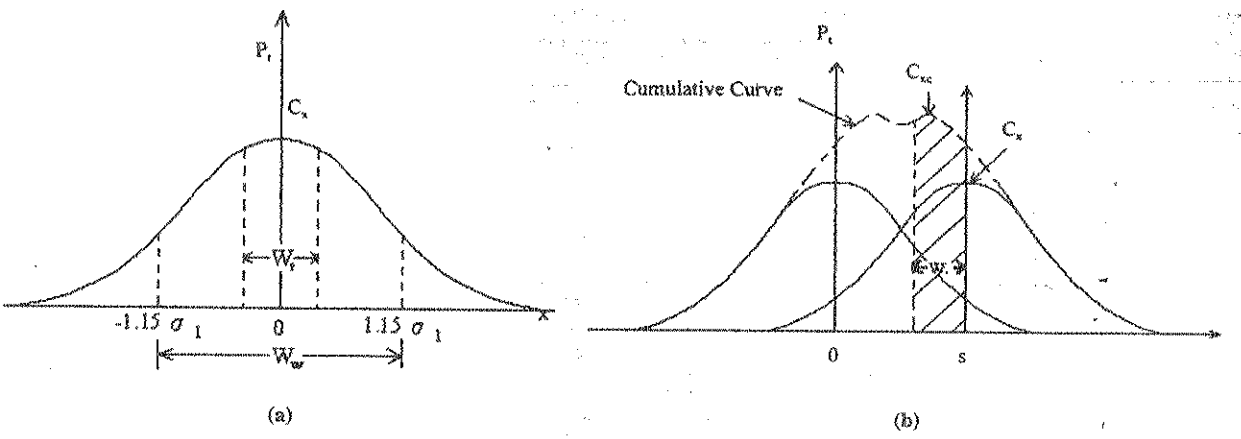

FIGURE 1 Concept of pass-to-coverage ratio: (*a*) theoretical normal distribution of aircraft traffic, and (*b*) general normal distribution for overlapping single wheels.

wheel spacing. The maximum ordinate (C_{xc}) will be twice as large as that of either single-wheel curve (C_x). Thus, the ratio of one aircraft pass to coverage will be reduced by half the original value.

$$P_c(x) = \frac{1}{\sigma_x\sqrt{2\pi}} e^{-\frac{1}{2}\left(\frac{x}{\sigma_x}\right)^2} + \frac{1}{\sigma_x\sqrt{2\pi}} e^{-\frac{1}{2}\left(\frac{x-s}{\sigma_x}\right)^2} \quad (2)$$

$$\text{P C} = \frac{1}{(C_{xc})(W_t)}$$

The P/C ratio concept was reexamined in this study. The P/C ratios reported in the conventional FAA design procedures for various gear assemblies and aircraft types are given in Table 1 (*3*). The wheel spacing and tire width of specific aircraft types were not clearly specified in the conventional FAA design methodology; thus, these were obtained from the LED–FAA program for all aircraft types in this study for consistency. The standard deviation of the lateral placement of wheel centerline was not clearly specified and was assumed to be 77.5 cm (30.5 in.) for all aircraft types. Customized functions were written by using the S-PLUS statistical package (*8*) to conduct this analysis, and the results are summarized in Table 1. The P/C ratios of B-777 airplanes were subsequently determined. Apparently, the aforementioned P/C ratio concept is indeed in very good agreement with what is described in the literature.

It was also noted that the concept of coverage, which includes only wheel passes that overlap one another within a pavement, is a rather crude application of cumulative damage concept. The effects of stresses other than the maximum were neglected, and the effect of the edge of a tire at 0 is assumed as detrimental as the effect of the tire centerline at 0, as shown in Figure 1(*a*). In addition, the location of the centerline of the lateral wheel load placement of each aircraft is considered to be coincident. This is not necessarily true and a further refinement is warranted (*6,9,10,11*). More detailed analyses were conducted and will be discussed later.

ESTIMATION OF CRITICAL EDGE STRESS FOR DESIGN

The conventional FAA pavement design curves were developed by using Westergaard edge loading analysis for rigid pavements. The edge loading stress was reduced by 25 percent to account for the effect of load transfer across the joints. This factor was chosen from test results and experience and is in use today. As coded in the R805FAA program, Equation 3 was adopted to determine the critical edge stress (σ_e) of the slab by using Pickett and Ray's influence charts and the concept of equivalent single-wheel load. The ratio of the concrete flexural strength (S_c) to the allowable slab tensile stress ($\sigma_a = 0.75 * \sigma_e$) is called a design factor (DF), analogous to a safety factor.

$$\sigma_e = \frac{P}{h^2}\left[\text{RC0} + \text{RC1} \times \ln(\ell) + \text{RC2} \times (\ln(\ell))^2\right] \quad (3)$$

$$\text{DF} = \frac{S_c}{0.75 * \sigma_e}$$

where

RC0, RC1, and RC2 = coefficients obtained by using influence charts for various aircraft types and provided along with the R805FAA program;
P = main landing gear load, lb;
σ_e = critical edge tensile stress, psi;
$\ell = (E * h^3/(12 * (1 - \mu^2) * k))^{0.25}$ = radius of relative stiffness, in.;
E = elastic modulus of the slab, psi;
k = modulus of subgrade reaction, psi/in.;
μ = Poisson's ratio; and
h or h_1 = slab thickness, in.

Note that this equation is applicable only in the U.S. customary system (English system). Proper adjustments to the coefficients should be made to use the equation with pertinent input variables in the metric system (SI system).

It is well understood that the classical solutions often fail to represent the actual pavement conditions because of certain simplifications and assumptions of the theory. With the help of a finite element (FE) computer program and today's high-speed computers, many important aspects of a pavement system may be more accurately and realistically determined. The literature has clearly shown the versatility and generality of FE programs for analyzing pavement structures (*12–15*). However, the difficulties of the required run time, the complexity of FE analysis, and the possibility of obtaining incorrect results due to the improper use of FE model often prevent it from being used in practical pavement design procedures.

TABLE 1 Reevaluation of Pass-to-Coverage Ratio for Different Aircraft Types

Aircraft Type	FAA P/C Ratio	No. of Wheels	Wheel Spacing, cm (in.)	Tire Width, cm (in.)	Calculated P/C Ratio
SINGLE WH-30	5.18	1	0	31.2 (12.30)	6.22
SINGLE WH-45		1	0	34.9 (13.75)	5.56
SINGLE WH-60		1	0	37.3 (14.7)	5.20
SINGLE WH-75		1	0	39.0 (15.37)	4.97
DUAL WH-50	3.48	2	50.8 (20)	27.6 (10.87)	3.71
DUAL WH-75		2	53.3 (21)	28.8 (11.35)	3.57
DUAL WH-100		2	58.4 (23)	29.5 (11.62)	3.53
DUAL WH-150		2	76.2 (30)	33.8 (13.31)	3.24
DUAL WH-200		2	86.4 (34)	34.9 (13.75)	3.25
DUAL TAN-100	3.68	4	50.8 (20)	22.5 (8.87)	4.55
DUAL TAN-200		4	53.3 (21)	27.6 (10.87)	3.73
DUAL TAN-300		4	66.0 (26)	31.9 (12.55)	3.34
DUAL TAN-400		4	76.2 (30)	34.9 (13.75)	3.14
C-130	4.15	2	0	42.4 (16.70)	4.58
L-1011	3.62	4	132.1 (52)	41.1 (16.17)	3.40
A-300-B2	3.51	4	88.9 (35)	33.2 (13.08)	3.45
A-300-B4	3.45	4	91.9 (36.2)	32.4 (12.77)	3.57
B-757	3.88	4	86.4 (34)	29.1 (11.46)	3.90
B-767	3.9	4	114.3 (45)	32.8 (12.91)	3.89
DC-10-10	3.64	4	137.2 (54)	37.8 (14.90)	3.80
DC-10-30	3.38	4	137.2 (54)	40.6 (15.99)	3.54
DC-10-30Belly		2	95.3 (37.5)	40.8 (16.05)	2.88
B-747-200	3.7	4	111.8 (44)	35.6 (14.03)	3.53
B-747-SP		4	110.0 (43.3)	34.1 (13.44)	3.66
B-777-200A	N/A	6	139.7 (55)	34.6 (13.63)	4.21
B-777-200B		6	139.7 (55)	34.6 (13.64)	4.21
B-777-200C		6	139.7 (55)	36.7 (14.44)	3.97

Note: The standard deviation is assumed as 77.5 cm (30.5 in.).

Nevertheless, the Portland Cement Association's thickness design procedure (or PCA method) is the most well-known and widely adopted mechanically based procedure for the thickness design of jointed concrete pavements for highways and streets based on the results of J-SLAB FE analysis (*16,17*). The PCA method has adopted the concept of cumulative fatigue damage and equivalent stress. As Lee et al. (*18*) indicated, PCA's equivalent stress was determined on the basis of a fixed slab modulus, a fixed slab length and width, and a constant contact area, wheel spacing, axle spacing, and aggregate interlock factor to simplify the calculations. The equivalent stress equation is applicable only in the U.S. customary system because of the nature of the stress prediction models originally developed.

To expand the applicability of the PCA's equivalent stress for different material properties, finite slab sizes, gear configurations, environmental effects (e.g., temperature differentials), and different unit systems, Lee et al. (*18*) developed prediction models for various stress adjustment factors by using the well-known ILLI-SLAB FE program (*19*). The ILLI-SLAB program's applicability for stress estimation was further verified by reproducing very favorable results to the test sections of Taiwan's second northern highway, the

AASHO Road Test, and the Arlington Road Test (*20*). Thus, the following equation may be used for the estimation of critical stresses along the longitudinal edge of the slab:

$$\sigma_e = \sigma_{we} * R_1 * R_2 * R_3 * R_4 * R_5 + R_T * \sigma_{ce}$$

$$\sigma_{we} = \frac{3(1+\mu)P}{\pi(3+\mu)h^2}\left[\ln\frac{Eh^3}{100ka^4} + 1.84 - \frac{4}{3}\mu + \frac{1-\mu}{2} + 1.18(1+2\mu)\frac{a}{\ell}\right] \quad (4)$$

$$\sigma_{ce} = \frac{CE\alpha\Delta T}{2} = \frac{E\alpha\Delta T}{2}\left\{1 - \frac{2\cos\lambda\cosh\lambda}{\sin 2\lambda\sinh 2\lambda}(\tan\lambda + \tanh\lambda)\right\}$$

where

σ_e = predicted critical edge stress, $[FL^{-2}]$;
σ_{we} = Westergaard's closed-form edge stress solution, $[FL^{-2}]$;
σ_{ce} = Westergaard–Bradbury's edge curling stress, $[FL^{-2}]$;
C = curling stress coefficient $[\lambda = B/((8^{0.5}) * \ell)]$;
B = finite slab length or width;
P = main landing gear load, $[F]$;
a = applied load radius, $[L]$;
α = thermal expansion coefficient, $[T^{-1}]$; and
ΔT = temperature differential through the slab thickness.

R_1 is an adjustment (or multiplication) factor, which represents the combined effect of several prediction models for different gear configurations including dual-wheel, tandem axle, and tridem axle. R_2, R_3, R_4, and R_5 are adjustment factors for finite slab length and width, a tied concrete shoulder, a widened outer lane, and a bonded-unbonded second layer, respectively. R_T is the adjustment factor for the combined effect of loading plus daytime curling. It should be emphasized that the proposed models were developed on the basis of the principles of dimensional analysis. All the mechanistic variables involved in the prediction models are dimensionally correct or dimensionless. Thus, the above equation is applicable to the U.S. customary system and the metric system. More detailed descriptions of the proposed prediction models for edge stress adjustments can be found in the literature (*18*).

The applicability of these prediction models for critical edge stress estimations is also reexamined in this study. The default characteristics of all aircraft types given in Table 1 were obtained from the LED–FAA program. The corresponding RC0, RC1, and RC2 values for each aircraft type were obtained from the R805FAA program, except for the B-777 airplanes. A wide variety of different pavement designs including h = 30.5–50.8 cm (12–20 in.), E = 27.6–41.3 GPa (4 million–6 million psi), and k = 27–108 MN/m³ (100–400 lb/in³) was chosen for the analysis. Critical edge stresses resulting from the main landing gear loads of different aircraft types on a very long slab were estimated by using Equations 3 and 4. In such a comparison, Equation 4 was reducing to $\sigma_e = \sigma_{we} * R_1$, because the effects of R_2, R_3, R_4, and R_5 are neglected and should have the same value of unity. Furthermore, the combined effect of loading plus curling was not considered here and thus R_T is equal to zero. As shown in Figure 2, the critical edge stresses obtained from the proposed prediction models (Equation 4) are indeed in very good agreement with those determined by using Equation 3, with only the exception of the A-300-B4 aircraft type. It is believed, however, that the corresponding coefficients of RC0 = 2.24009, RC1 = −1.18694, and RC2 = 0.314165 for the A-300-B4 aircraft type were mistakenly recorded in the R805FAA program. Thus, Equation 4 will be used as a supplemental equation to the original FAA Equation 3 for the estimation of critical edge stresses of A-300-B4 and B-777 aircraft types in the subsequent analyses.

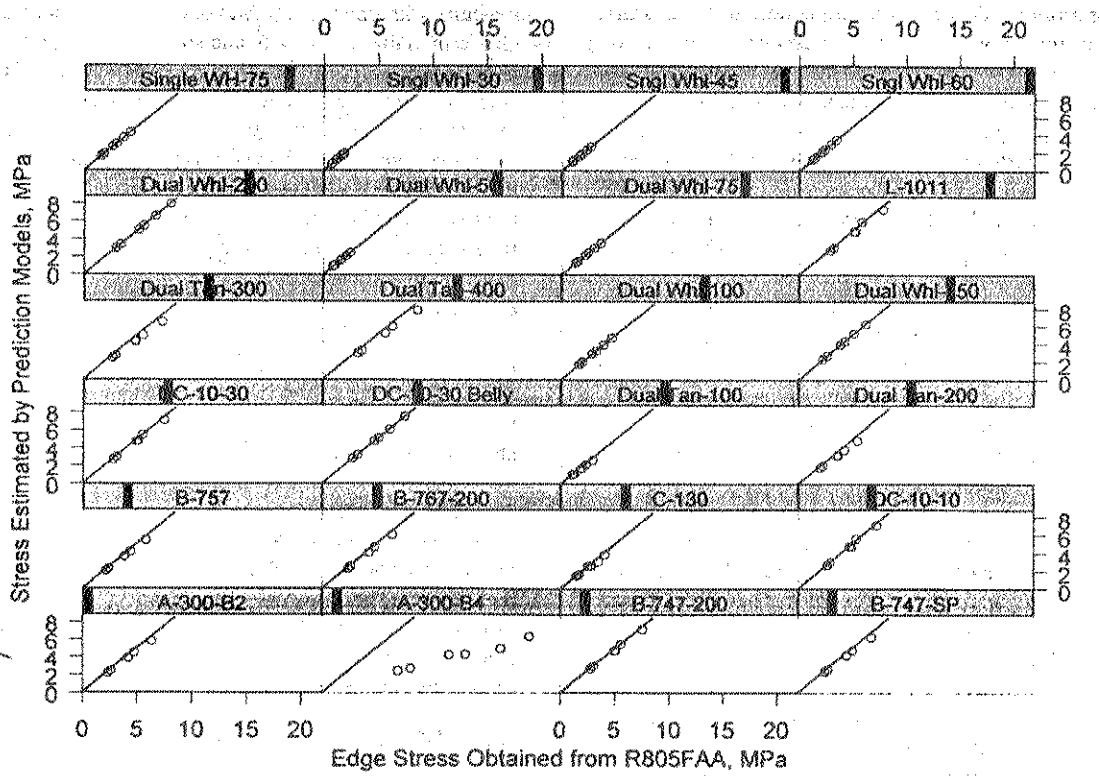

FIGURE 2 Verification of proposed stress prediction models.

CONVERSION OF DIFFERENT AIRCRAFT TYPES AND DEPARTURES

Because the traffic forecast is a mixture of a variety of aircraft having different landing gear types and weights, the "design aircraft" concept was introduced to account for the effects of all traffic in the conventional FAA design methodology. Each aircraft type in the forecast should be checked to determine the required pavement thickness by using the corresponding design curve with the forecasted annual departures. The design aircraft is the one that produces the greatest pavement thickness and is not necessarily the heaviest aircraft in the forecast. All aircraft must be converted to the same landing gear type as the design aircraft. Conversion factors, which represent "an approximation of the relative fatigue effects of different gear types," have been established for both flexible and rigid pavements (*3*). After the aircraft have been grouped into the same landing gear configuration, the conversion to equivalent annual departures of the design aircraft is determined by

$$\log R_1 = \log R_2 \times \sqrt{\frac{W_2}{W_1}} \tag{5}$$

where

R_1 = equivalent annual departures by the design aircraft;
R_2 = annual departures expressed in design aircraft landing gear;
W_1 = wheel load of the design aircraft; and
W_2 = wheel load of the aircraft in question.

Wheel load for wide body aircraft is taken as the wheel load for a 136 100-kg (300,000-lb) dual tandem aircraft for equivalent annual departure calculations.

Commonly, these equivalencies for the relative fatigue effects of different gear types are defined by a simple ratio of the evaluated total repetitions for the two loadings being compared for a selected pavement structure. However, it is noted that the load equivalencies, presently determined by the aforementioned conversion factors and Equation 5, are not single valued and may vary widely for different levels of aircraft departures in this study. This conclusion is similar to the statement by Ahlvin (*9*) that "any simple ratio will be different for different magnitudes of load repetitions so that the adopted practice is arbitrary and unverified." Thus, FAA (*3*) has also indicated that "much more precise and theoretically rigorous factors could be developed for different types and thickness of pavements."

Consequently, the conventional "design aircraft" concept, conversion factors for different landing gear types, and Equation 5 have been replaced by the concept of cumulative damage factor (CDF) in the new LED–FAA design methodology (*4*). The cumulative damage effects of multiple aircraft types and departures are accounted for by using Miner's hypothesis. This approach is more mechanistically based and will result in a single valued factor to represent the relative fatigue effects of different aircraft types for a given pavement structure. This single valued factor will vary widely for different aircraft loads, gear configurations, and properties of pavement structure but not the magnitude of load repetitions. Several practical examples showing that such a conversion is more theoretically rigorous than the conventional FAA approach were conducted in this study (*5*). Also note that through the use of the CDF concept, the conversion of different aircraft types and departures to equivalent annual departures of a specific aircraft type is no longer necessary and thus will not be further discussed in this paper.

FATIGUE RELATIONSHIP AND THICKNESS DESIGN CRITERIA

The conventional FAA thickness design methodology was based on an earlier fatigue curve developed by the Corps of Engineers from test track data and observation of full-scale test pavements. The fatigue curve originally adopted a bilinear relationship between a DF and the number of load repetitions (in terms of coverages, C) at the specified failure criteria. However, no explicit fatigue relationship is available elsewhere in the literature (*3*). The method presently adopted for the determination of minimum required slab thickness for design is based on the concept of basic slab thickness. A DF of 1.3 was chosen to determine the allowable slab tensile stress for 5,000 coverages. The thickness of pavement required to sustain 5,000 coverages of the design loading is considered to be the basic thickness (or 100 percent thickness). The required design thickness for the expected 20-year coverage levels is determined by the product of the basic thickness (h_1) and the percent thickness (or relative thickness, RH). The pertinent equations for design are summarized as follows:

$$\sigma_e = \frac{S_c}{1.3 * 0.75}$$

$$h_1 = \left[\left(\mathrm{RC0} + \mathrm{RC1} \times \ln(\ell) + \mathrm{RC2} \times (\ln(\ell))^2\right) \times \left(\frac{P}{\sigma_e}\right)\right]^{0.5} \tag{6}$$

$$\mathrm{RH} = \begin{cases} 1 + 0.15603 * (\log(C) - 3.69897) & \text{if } C > 5000 \\ 1 + 0.07058 * (\log(C) - 3.69897) & \text{if } C < 5000 \end{cases} \tag{7}$$

Equation 7 was identified under this study by finally checking into the source code of the R805FAA program, because it was often presented in a graphical form elsewhere (*3*). For any given pavement structure with known slab thickness, concrete modulus of rupture, elastic modulus of the slab, and subgrade modulus, the allowable number of load repetitions (in terms of coverages) of a specific aircraft and wheel load may be determined through a very simple back-calculation process. Thus, the above equations are analogous to a fatigue relationship. However, it is worth mentioning that the relationship between a DF and coverages derived from the above equations is not a unique curve any longer. As shown in Figure 3(*a*), the fatigue curves showing a bilinear relationship and coinciding at the point of DF = 1.3 and C = 5,000 are obtained for different sets of P, E, h, k, and S_c values, for example.

Rollings and Witczak (*21*) developed a structural deterioration model for rigid airfield pavements that predicts performance in terms of a structural condition index (SCI), a DF, the coverages at the onset of structural deterioration (CO), and the coverages at absolute failure (CF). The SCI is derived from the pavement condition index (PCI), considering the distresses associated with tensile fatigue loading only, and is on a scale of from 0 to 100. The DF is defined as the ratio of flexural strength of concrete (S_c) and the critical tensile stresses (σ) calculated by using the layered elastic pavement model. The basic fatigue relationship used to find the number of coverages (C) to failure in the LED–FAA program (*4,21*) is as follows. Failure is defined as the number of coverages (C_{80}) to reduce the pavement SCI to 80 at any given value of DF or S_c/σ.

$$\mathrm{SCI} = \frac{\mathrm{DF} - 0.2967 - (0.3881 + 0.000039 * \mathrm{SCI})\log(C)}{0.002269} \tag{8}$$

$$\mathrm{DF} = 0.4782 + 0.3912 * \log(C_{80})$$

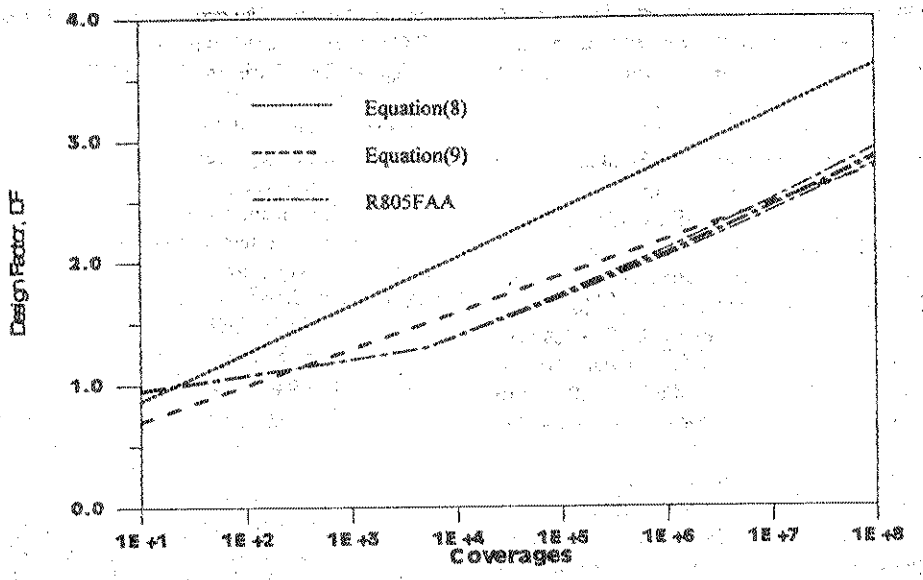

(a)

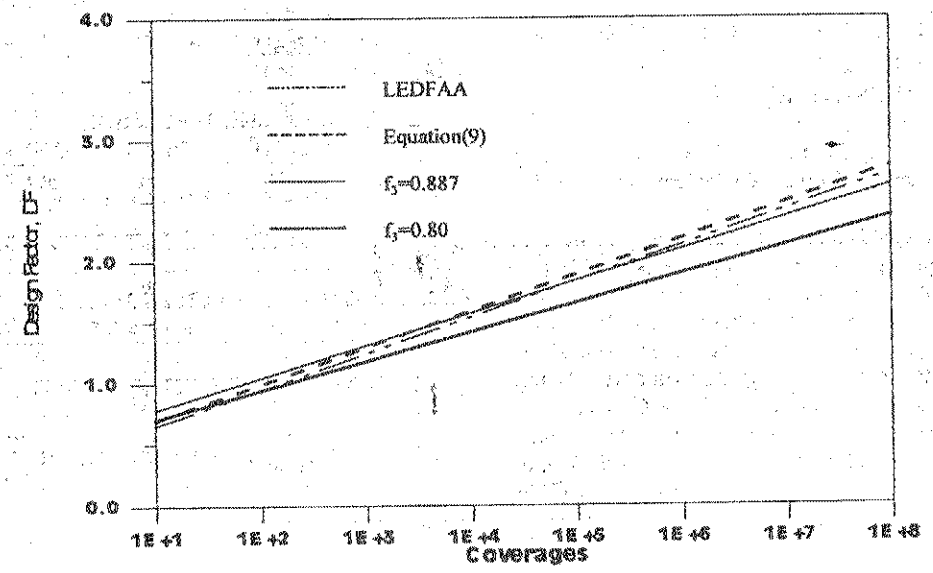

(b)

FIGURE 3 Comparison of fatigue relationships for rigid airfield pavement design.

Gucbilmez and Yuce (22) reanalyzed the Corps of Engineers accelerated traffic data and provided an alternative rigid airfield pavement deterioration relationship using stresses calculated by the Westergaard edge loading idealization. This relationship can be used to determine the expected structural condition of the pavement at a specified level of coverages or vice versa for pavements with joints capable of load transfer. The DF is defined by DF = S_c/(0.75 * σ_c) as usual. The equation is given as follows:

$$SCI = \frac{100 * \log(C) - 320.61558DF + 56.4417}{0.20903DF - 0.99336} \quad (9)$$

$$DF = 0.40289 + 0.29644 * \log(C_{80})$$

Figure 3(*a*) shows a comparison of the conventional FAA and the basic LED–FAA fatigue equations with the fatigue curve given in Equation 9. It is noted that the fatigue curve obtained by Gucbilmez and Yuce (22) performs similarly with the conventional FAA fatigue curve given by Equations 6 and 7, although the specified failure criteria may be different. Generally speaking, the fatigue equation, Equation 9, requires a thicker pavement than the conventional FAA curve for a given coverage level above 1,000.

The coverages at failure (C_{80}) obtained from both fatigue equations, Equations 8 and 9, were implicitly tied to the manner in which critical tensile stress, or consequently the DF, was determined. To make the layered elastic design procedure compatible with the conventional

FAA thickness design procedure, an adjustment is made to the calculated layered elastic interior stress to provide an equivalent edge stress. The subgrade is assumed to be infinite in thickness and is characterized by either an elastic modulus (E) or a modulus of subgrade reaction (k-value) in the current LED–FAA program. If a k-value is specified, it is converted to an equivalent E-value by using a logarithmic relationship: $\log E = 1.415 + 1.284 \log k$.

Fatigue failure expressed in terms of a CDF by using Miner's hypothesis is adopted in the new LED–FAA thickness design approach. CDF is the amount of the consumed structural fatigue life and is expressed as the summation of the ratio of applied load repetitions to allowable load repetitions to failure. The LED–FAA program automatically calculates the damaging effects of each aircraft in the traffic mix. When the damaging effects of all aircraft sum to a value of 1.0, the design conditions have been satisfied and the required slab thickness is determined.

These comparisons show that a scaling factor is required to reduce the conservatism of the basic LED–FAA fatigue relationship. It is also noted that in the current LED–FAA method, a scaling factor of 0.753 is applied to stresses used to compute the DF. As shown in Figure 3(b), the resulting fatigue curve is similar to the conventional FAA curves and is slightly less conservative than the relationship based on the Gucbilmez and Yuce study.

INVESTIGATION OF TENTATIVE MODIFICATION ALTERNATIVES

Currently, the change from plate theory to layered elastic theory or the use of the two cannot resolve the problem for the design of rigid airfield pavements. The adoption of both the new LED–FAA method and the conventional FAA design methodology at the same time for pavements with or without B-777 airplanes is cumbersome and highly undesirable. As mentioned, the coverages at failure obtained from the fatigue curves were implicitly tied to the manner in which critical tensile stress was determined. The load magnitude and load repetitions to failure are certainly interrelated with the material properties of a given pavement structure. The P/C concept may adequately represent the lateral placement frequency of the centerline of one wheel on the aircraft with a specific tire width (W_t). Its extension to aircraft having multiple wheels also appears reasonable. However, the use of the P/C concept is in fact a rather crude application of cumulative damage concept. As shown in Figure 1(a), the P/C concept is based on the assumption that the effect of the edge of a tire at 0 is as detrimental as the effect of the tire centerline at 0. In other words, the P/C concept also implies that maximum tensile stress should be used throughout when the centerline location of the lateral wheel load placement (L_c) falls within this tire print area, as shown in Figure 4. Figure 4 is obtained by assuming a standard deviation of 77.5 cm and a tire width of 38.1 cm, for example. Thus, the well-recognized effect of stress reduction due to the wandering of the L_c, moving away from the maximum tensile stress location, is totally neglected by the P/C concept. The P/C concept is indeed embedded with a very conservative means for estimating the cumulative fatigue damages of each aircraft type, and a further refinement is warranted.

To help formulate a unified approach for the design of rigid airfield pavements, tentative modification alternatives are further investigated as follows. The effect of edge stress reduction due to the wandering of the L_c can be treated as the effect of a widened outer lane in the literature. As a supplement to Equation 4, the following prediction model was proposed by Lee et al. (5) to account for the stress reduction due to the width of a widened outer lane (D_0). The L_c as previously defined in Figure 4 is equivalent to D_0 in Equation 10.

$$R_4 = 0.61711 + 0.15373\Phi_1 + 0.02504\Phi_2$$

$$\Phi_1 = \begin{cases} 0.693 + 1.279(A1) + 0.369(A1)^2 \\ \quad + 0.037(A1)^3 \qquad \text{if } A1 \le -2.5 \\ \\ 2.839 + 8.234(A1) + 8.158(A1)^2 \\ \quad + 3.608(A1)^3 + 0.576(A1)^4 \qquad \text{if } A1 > -2.5 \end{cases}$$

$$\Phi_2 = \begin{cases} -2.285 + 5.921(A2) - 6.001(A2)^2 \\ \quad + 7.743(A2)^3 \qquad \text{if } A2 \le 0.5 \\ \\ -3.008 + 4.693(A2) + 4.334(A2)^2 \\ \quad - 2.167(A2)^3 \qquad \text{if } A2 > 0.5 \end{cases}$$

$$A1 = -0.98868\left(\frac{D_0}{\ell}\right) - 0.12214\left(\frac{a}{\ell}\right) - 0.08717\left(\frac{D_0}{a}\right) \tag{10}$$

$$A2 = 0.19802\left(\frac{D_0}{\ell}\right) + 0.98019\left(\frac{a}{\ell}\right) + 0.00305\left(\frac{D_0}{a}\right)$$

Limits: $0.1 \le \frac{a}{\ell} \le 0.4,\ 0 \le \frac{D_0}{\ell} \le 2$

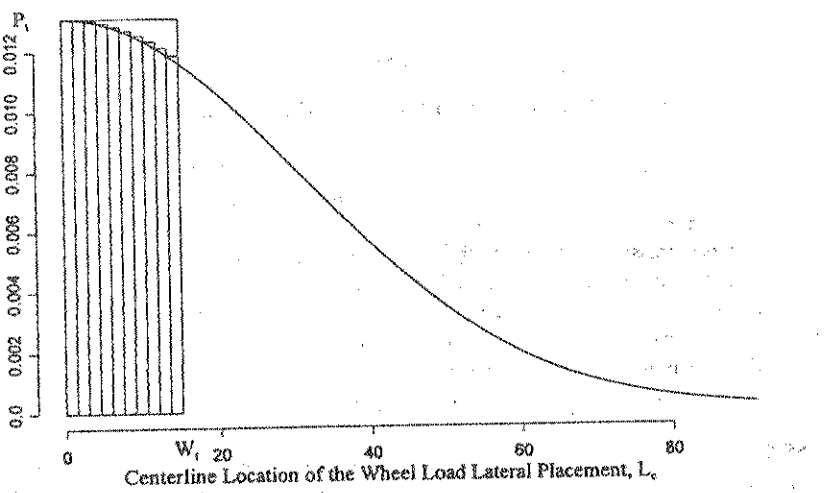

FIGURE 4 Lateral placement of centerline location of wheel load.

Determination of Equivalent Stress Factor (f_3)

The Corps of Engineers accelerated traffic data provided by Gucbilmez and Yuce (22) was reanalyzed in this study. As given in Table 2, the coverages at the onset of structural deterioration (CO), the coverages at initial failure (CI), the coverages at absolute failure (CF), and the DF are obtained. Critical edge stresses also can be determined by the proposed model given by Equation 4 or by $\sigma_e = \sigma_{we} * R_1$, and very favorable agreements with those reported by Gucbilmez and Yuce are observed. The radius of the wheel load (a) and the tire width (W_t) are obtained by using the relation $1.273(\pi a^2) = 1.6 (W_t)^2$, similar to that used in the LED–FAA program. More detailed descriptions of the data and original development of Equation 9 can be found in the literature (22).

TABLE 2 Reanalysis of Corps of Engineers Accelerated Traffic Test Data

item	quality	CO	CF	CI	DF	a (cm)	Wt (cm)	P/C	f_3
A1.60	A	13	59	45	0.855	36.16	57.17	3.31	0.808
B2.66L	B			187	0.948	28.06	44.37	4.11	0.826
B1.66L	A	3	96	35	0.679	36.16	57.17	3.31	0.796
C2.66S	A	48	636	200	0.934	28.06	44.37	4.11	0.826
C1.66S	A	13	92	44	0.667	36.16	57.17	3.31	0.795
D1.66	A	6	104	33	0.679	36.16	57.17	3.31	0.796
E2.66M	B			430	1.081	28.06	44.37	4.11	0.835
E1.66M	A	50	212	77	0.779	36.16	57.17	3.31	0.806
F1.80	B			111	0.967	36.16	57.17	3.31	0.835
K2.100	B			72	1.004	36.16	57.17	3.31	0.859
N1.86	A	105	285	150	1.096	36.16	57.17	3.31	0.840
N2.86	A	6	32	9	0.782	46.46	73.45	2.58	0.809
O1.106	A	347	1605	573	1.367	36.16	57.17	3.31	0.862
O2.106	A	41	155	72	0.959	46.46	73.45	2.58	0.830
P1.812	A	244	1148	262	1.078	36.16	57.17	3.31	0.835
P2.812	B			6	0.782	46.46	73.45	2.58	0.806
Q1.102	B			1390	1.484	36.16	57.17	3.31	0.865
Q2.102	A	36	237	57	1.055	46.46	73.45	2.58	0.833
U1.60	A	85	529	88	0.951	36.16	57.17	3.31	0.819
E-6	A	1343	13083	2204	1.383	54.65	86.40	2.25	0.872
M-1	A	68	379	134	1.005	23.52	37.19	2.98	0.873
M-2	A	1693	6781	2204	1.330	23.52	37.19	2.98	0.892
-	B			18	0.596	26.13	41.32	2.82	0.810
59	B			7600	1.246	23.42	37.02	3.17	0.887
60	B			1674	1.114	23.42	37.02	3.17	0.856
61	B			3867	1.355	23.42	37.02	3.17	0.873
62	B			10082	1.705	23.42	37.02	3.17	0.888
72	B			9680	1.714	23.41	37.01	2.99	0.912
73	A	662	7078	2115	1.365	23.41	37.01	2.99	0.901
1-C5	A	150	939	221	0.880	24.09	38.08	2.98	0.833
2-DT	A	128	477	95	0.896	20.63	32.61	3.86	0.873
3-DT	A	177	959	205	1.033	20.63	32.61	3.86	0.883
2-C5	A	292	783	344	1.133	24.09	38.08	2.98	0.834
4-DT	A	227	1092	320	1.208	20.63	32.61	3.86	0.865
3-200	A	939	4269	3215	1.443	23.42	37.02	3.40	0.892
4-200	A	1188	5741	4660	1.474	23.42	37.02	3.40	0.891

Note: Item name is the same item designation used by Gucbilmez and Yuce (1995). If the test item is suitable for use in the analysis of CO, CF, and CI, that item is referred to as "quality" class A. Class B is suitable for use in the analysis of CI only. Assuming $1.273(\pi a^2) = 1.6 (W_t)^2$.

The traffic at failure in terms of coverages assigned to each of the test pavements was for one type load and is implicitly tied to the manner in which the traffic was applied (*10*). The P/C ratio of each original test item was calculated by using Equations 1 and 2. The fatigue relationships developed for CO, CI, and CF as functions of DF are labeled as models 1 to 3 in Table 3, where SEE is the standard error of estimate, R^2 is the coefficient of determination, and N is the number of observations. These three models are identical to those reported in Gucbilmez and Yuce's paper and are the basic fatigue relationships used to develop Equation 9. In an attempt to investigate the possibility of the dismissal of the P/C concept, models 4 through 6 are developed for the passes at the onset of structural deterioration (PO), at initial failure (PI), and at absolute failure (PF) as functions of DF. Comparison between models 1 to 3 and models 4 to 6, respectively, indicates that the inclusion of P/C concept slightly improves the fatigue relationships and corresponding regression statistics. It still is worth the effort to continuously use the P/C concept, although the slopes are approximately the same and the mean difference of the intercepts in these models is about 0.14, which may be represented by 0.3 * log(average P/C) approximately.

Thus, research efforts are focused on the determination of "equivalent stress factor" (f_3) when the centerline location of the lateral wheel load placement (L_c) falls within the full tire print, as shown in Figure 4, which is also compatible with the P/C concept. The equivalent stress factor (f_3) is often referred to as a value of 0.894 throughout the PCA thickness design procedures for the determination of equivalent stress (*18*). The f_3 factor is defined in this study as the stress adjustment factor (or reduction factor) based on the equivalency of the cumulative fatigue damages to account for the lateral wandering effect of the L_c within the full tire print area and may be determined by the following computerized procedures:

1. Select each test item or aircraft type, gear configurations, and a standard deviation of the lateral distribution; input other pertinent design parameters such as slab modulus, subgrade modulus, concrete flexural strength, and slab thickness.
2. Assume a normally distributed aircraft pass data set (n_i) in smaller intervals, say 10 intervals, of the specified wheel width (W_t), as shown in Figure 4.
3. Calculate the critical edge stress by using Equations 4 and 10 for each interval, that is, $\sigma_e = \sigma_{ne} * R_1 * R_4$.
4. Calculate the corresponding allowable number of load repetitions (N_i) in terms of coverages for each interval using the fatigue relationship given by Equation 9.
5. Calculate the cumulative fatigue damage $\Sigma(n_i/N_i)$ for the given aircraft pass data within the full tire print.
6. Determine the maximum edge stress (σ_{max}) or the critical edge stress of the first interval.
7. Determine the equivalent allowable number of load repetitions (N_{eq}) by calculating the ratio of $\Sigma(n_i)$ and $\Sigma(n_i/N_i)$, assuming all aircraft passes applied on the maximum edge stress location.
8. Backcalculate the equivalent edge stress (σ_{eq}) by using the obtained N_{eq} value and Equation 9.
9. The equivalent stress factor (f_3) is determined by the ratio of σ_{eq} and σ_{max}.
10. Repeat steps 1–9 for each test item or aircraft type.

The equivalent stress factor (f_3) determined in such a manner is more mechanistically based in attempts to represent an approximation of equivalent cumulative fatigue damages. The f_3 factor may vary widely for different aircraft types, gear configurations, lateral distributions, and other pertinent design parameters. This proposed procedure has been further verified by producing an f_3 value of 0.88 to 0.89, which is very close to 0.894 used by the PCA method, based on PCA's fatigue relationship and simplifications of other pertinent design parameters (*5*).

Alternative Structural Deterioration Relationship for Design

The f_3 value of each of the test items was calculated on the basis of the proposed procedure and is given in Table 2. An equivalent design factor (EDF) is defined by EDF = $S_c/(0.75 * \sigma_e * f_3)$ to account for the reduction of critical edge stress. Similarly, fatigue relationships are developed for CO, CI, and CF as functions of EDF and are listed as models 7 through 9 in Table 3. Models 10 through 12 are developed for PO, PI, and PF as functions of EDF in a similar fashion.

Models 7 through 9 are proposed for subsequent analyses in this study. The structural deterioration of a pavement slab at a given coverage level defined by Gucbilmez and Yuce (*22*) is as follows:

TABLE 3 Alternative Structural Deterioration Relationships

Model No.	Tentative Fatigue Equations	SEE	R^2	N
#1	DF = 0.4561 + 0.2928*log(CO)	0.108	0.822	24
#2	DF = 0.3470 + 0.3013*log(CI)	0.125	0.818	36
#3	DF = 0.1760 + 0.3119*log(CF)	0.122	0.775	24
#4	DF = 0.3171 + 0.2894*log(PO)	0.114	0.804	24
#5	DF = 0.2124 + 0.2953*log(PI)	0.131	0.800	36
#6	DF = 0.0338 + 0.3074*log(PF)	0.127	0.755	24
#7	EDF = 0.6421 + 0.2920*log(CO)	0.119	0.793	24
#8	EDF = 0.5266 + 0.3037*log(CI)	0.136	0.792	36
#9	EDF = 0.3697 + 0.3086*log(CF)	0.134	0.735	24
#10	EDF = 0.5056 + 0.2879*log(PO)	0.125	0.771	24
#11	EDF = 0.3911 + 0.2976*log(PI)	0.142	0.774	36
#12	EDF = 0.2319 + 0.3032*log(PF)	0.140	0.712	24

$$SCI = 100\left(\frac{\log(CF/C)}{\log(CF/CO)}\right) \tag{11}$$

where C is the coverage level at which the SCI is to be calculated. The following fatigue relationship is obtained by solving models 7 and 9 for CO and CF and substituting the results into Equation 11. The C_{80} is the coverages to reduce the pavement SCI from 100 to 80.

$$SCI = \frac{100 * \log(C) - 324.044(EDF) + 119.799}{0.184217(EDF) - 1.00098} \tag{12}$$

$$EDF = 0.5900 + 0.2952 * \log(C_{80})$$

$$DF = f_3 * [0.5900 + 0.2952 * \log(C_{80})]$$

The sensitivity analysis of the f_3 factor was conducted and is summarized in Table 4. Generally speaking, the f_3 factor increases when slab thickness (h), subgrade modulus (k), or concrete modulus of rupture (S_c), or all three, increase. The f_3 factor is not very sensitive to the increase in slab modulus (E); however, the f_3 value decreases when the tire width (W_t) increases. The structural deterioration relationship given by Equation 12 also is compared with the fatigue curves discussed earlier. As shown in Figure 3, the fatigue curve labeled f_3 = 0.887, which is the average value obtained from Table 4, performs similarly to that defined by Equation 9. A relative low value of f_3 = 0.80 was chosen and the corresponding fatigue curve is plotted in Figure 3(b) just to show how differently the proposed model will perform. The fatigue curve labeled as f_3 = 0.80 requires the least slab thickness.

TABLE 4 Sensitivity Analysis of Equivalent Stress Factor (f_3)

Aircraft Type	h=30.48 cm (12 in.)	h=40.64 cm (16in.)	h=50.8 cm (20 in.)	k=135 MPa/m (500 pci)	Sc= 5.5 MPa (800 psi)	E=41.3 GPa (6 Mpsi)
SINGLE WH-30	0.931	0.954	0.967	0.936	0.942	0.929
SINGLE WH-45	0.911	0.938	0.954	0.917	0.923	0.910
SINGLE WH-60	0.895	0.925	0.944	0.900	0.908	0.894
SINGLE WH-75	0.882	0.914	0.934	0.886	0.895	0.881
DUAL WH-50	0.920	0.943	0.958	0.926	0.931	0.918
DUAL WH-75	0.899	0.926	0.943	0.904	0.910	0.898
DUAL WH-100	0.884	0.912	0.931	0.887	0.896	0.884
DUAL WH-150	0.865	0.895	0.916	0.867	0.876	0.865
DUAL WH-200	0.851	0.881	0.903	0.850	0.862	0.853
DUAL TAN-100	0.916	0.937	0.951	0.924	0.926	0.913
DUAL TAN-200	0.881	0.906	0.923	0.888	0.892	0.880
DUAL TAN-300	0.864	0.890	0.908	0.872	0.875	0.864
DUAL TAN-400	0.852	0.878	0.897	0.859	0.863	0.852
C-130	0.840	0.874	0.898	0.838	0.851	0.842
L-1011	0.850	0.878	0.898	0.856	0.863	0.849
A-300-B2	0.870	0.895	0.913	0.879	0.882	0.868
A-300-B4	0.869	0.896	0.914	0.872	0.881	0.868
B-757	0.879	0.903	0.920	0.887	0.890	0.877
B-767	0.870	0.895	0.913	0.877	0.882	0.868
DC-10-10	0.858	0.885	0.903	0.864	0.870	0.857
DC-10-30	0.855	0.882	0.901	0.862	0.867	0.853
DC-10-30Belly	0.848	0.880	0.903	0.849	0.860	0.849
B-747-200	0.859	0.885	0.903	0.866	0.870	0.858
B-747-SP	0.865	0.891	0.909	0.872	0.877	0.864
B-777-200A	0.854	0.878	0.895	0.862	0.865	0.853
B-777-200B	0.846	0.870	0.887	0.851	0.856	0.847
B-777-200C	0.839	0.863	0.880	0.843	0.848	0.839
Average	0.872	0.899	0.917	0.878	0.884	0.872

Note: The standard deviation is assumed as 77.5 cm (30.5 in.). The basic input parameters are: h=30.48 cm (12 in.), k=54 MPa/m (200 pci), Sc= 4.48 MPa (650 psi), E=27.6 GPa (4 Mpsi)

overall. All the analyses were conducted by using the S-PLUS statistical analysis software. The proposed approach has also been implemented in a highly user-friendly computer program (TKUAPAV) (6) using the Microsoft Visual Basic software package (23).

CONCLUSIONS

Many research findings and conclusions can be obtained from this study. First, the original P/C concept was reexamined and the P/C ratio of the B-777 airplane was determined. Prediction models for the estimation of critical edge stresses were proposed and verified. The proposed models were developed on the basis of the principles of dimensional analysis and thus are applicable to both the U.S. customary system and the metric system. The problems and difficulties of the conventional FAA method in the conversions of different aircraft types and departures are identified. The concept of CDF is used to account for the combined damage effects of different aircraft types and departures.

Comparison of the conventional FAA and the basic LED–FAA fatigue relationships with the fatigue curve obtained by Gucbilmez and Yuce was conducted. These comparisons show that a scaling factor is required to reduce the conservatism of the basic LED–FAA fatigue relationship. It is noted that in the current LED–FAA method, a scaling factor of 0.753 is applied to stresses used to compute the DF. The resulting fatigue curve is similar to the conventional FAA curves and is slightly less conservative than the relationship based on the Gucbilmez and Yuce study.

The well-recognized effect of stress reduction due to the wandering of the centerline location of the lateral wheel load placement (L_c), moving away from the maximum tensile stress location, is totally neglected by the use of the P/C concept. Thus, the Corps of Engineers accelerated traffic data provided by Gucbilmez and Yuce (22) were reanalyzed in this study. An equivalent stress factor (f_3) based on the equivalency of the cumulative fatigue damages to account for the lateral wandering effect of the L_c within the full tire print area was introduced. An EDF is also defined to account for the reduction of critical edge stress. The alternative structural deterioration relationship given by Equation 12 is obtained. This fatigue relationship is in very good and very reasonable agreement with the performance trend of the existing fatigue curves.

The f_3 factor may vary widely for different aircraft types, gear configurations, lateral distributions, and other pertinent design parameters. The sensitivity analysis of the f_3 factor was conducted. Generally speaking, the f_3 value decreases when the tire width (W_t) increases. The proposed approach has been implemented in a user-friendly computer program (TKUAPAV) for practical trial applications (6). Further investigations and verification should be conducted in attempts to provide a more economic and maintenance-free design of rigid airfield pavements.

ACKNOWLEDGMENTS

This research work was sponsored by the National Science Council, Taiwan, Republic of China. The financial support provided by the Center for East Asian and Pacific Studies at the University of Illinois at Urbana-Champaign during the summer visiting study is gratefully acknowledged.

REFERENCES

1. Westergaard, H. M. Stresses in Concrete Runways in Airports. *HRB Proc.*, Vol. 19, 1926, pp. 192–202.
2. Burmister, D. M. The Theory of Stresses and Displacements in Layered Systems and Applications to the Design of Airport. *HRB Proc.*, Vol. 23, 1943, pp. 126–144.
3. *Airport Pavement Design and Evaluation.* Advisory Circular 150/5320-6D, Federal Aviation Administration, 1995.
4. *Airport Pavement Design for the Boeing 777 Airplane.* Advisory Circular 150/5320-16. Federal Aviation Administration, 1995.
5. Lee, Y. H., S. T. Yen, and P. K. Cheng. *Development of a New Thickness Design Procedure for Rigid Airfield Pavements.* Final Report NSC87-2218-E-032-007. National Science Council, Taiwan, R.O.C., 1998 (in Chinese).
6. Ahlvin, R. G., et al. *Multiple-Wheel Heavy Gear Load Pavement Tests.* AFWL-TR-70-113, Vol. I–IV. Air Force Weapons Laboratory, Kirtland AFB, New Mexico, 1971.
7. HoSang, V. A. *Field Survey and Analysis of Aircraft Distribution on Airport Pavements.* Report FAA-RD-74-36. Federal Aviation Administration, 1975.
8. *S-PLUS User's Guide,* Version 4.0. MathSoft, Inc. Seattle, Wash., 1997.
9. Ahlvin, R. G. *Origin of Developments for Structural Design of Pavements.* Report GL-91-26. U.S. Army Corps of Engineers, 1991.
10. Parker, F., Jr., W. R. Barker, R. C. Gunkel, and E. C. Odom. *Development of a Structural Design Procedure for Rigid Airport Pavements.* Report FAA-RD-77-81, WES-TR-GL-79-4. Federal Aviation Administration, 1979.
11. Ahlvin, R. G., and J. W. Hall. *Reanalysis of Multiple-Wheel Landing Gear Traffic Tests.* U.S. Army Engineer Waterways Experiment Station, 1992.
12. Ioannides, A. M. *Analysis of Slabs-on-Grade for a Variety of Loading and Support Conditions.* Ph.D. thesis. University of Illinois, Urbana, 1984.
13. Kuo, C. M., K. T. Hall, and M. I. Darter. Three-Dimensional Finite Element Model for Analysis of concrete Pavement Support. In *Transportation Research Record 1505,* TRB, National Research Council, Washington, D.C., 1995, pp. 119–127.
14. Chen, D-H., M. Zaman, J. Laguros, and A. Soltani. Assessment of Computer Programs for Analysis of Flexible Pavement Structure. In *Transportation Research Record 1482,* TRB, National Research Council, Washington, D.C., 1995, pp. 123–133.
15. Hjelmstad, K. D., J. Kim, and Q. H. Zuo. Finite Element Procedures for Three-Dimensional Pavement Analysis. *Proc., Aircraft/Pavement Technology: In the Midst of Change,* ASCE Airfield Pavement Conference, Seattle, Wash., 1997.
16. *The Design for Concrete Highway and Street Pavements.* Portland Cement Association, Skokie, Ill., 1984.
17. Tayabji, S. D., and B. E. Colley. *Analysis of Jointed Concrete Pavement.* Report FHWA-RD-86-041. FHWA, U. S. Department of Transportation, 1986.
18. Lee, Y.-H., J.-H. Bair, C.-T. Lee, S.-T. Yen, and Y.-M. Lee. Modified Portland Cement Association Stress Analysis and Thickness Design Procedures. In *Transportation Research Record 1568,* TRB, National Research Council, Washington, D.C., 1997, pp. 77–88.
19. Korovesis, G. T. *Analysis of Slab-on-Grade Pavement Systems Subjected to Wheel and Temperature Loadings.* Ph.D. thesis. University of Illinois, Urbana-Champaign, 1990.
20. Lee, Y.-H., S.-T. Yen, C.-T. Lee, J.-H. Bair, and Y.-M. Lee. Development of New Stress Analysis and Thickness Design Procedures for Jointed Concrete Pavements. *Proc., 6th International Purdue Conference on Concrete Pavement—Design and Materials for High Performance.* Purdue University, West Lafayette, Ind., 1997, pp. 39–62.
21. Rollings, R. S., and M. W. Witczak. Structural Deterioration Model for Rigid Airfield Pavements. *Journal of Transportation Engineering,* Vol. 116, No. 4, 1990, pp. 479–491.
22. Gucbilmez, E., and R. Yuce. Mechanistic Evaluation of Rigid Airfield Pavements. *Journal of Transportation Engineering,* Vol. 121, No. 6, 1995, pp. 468–475.
23. *Microsoft Visual Basic. Programmer's Guide and Language Reference.* Version 5.0. Microsoft Taiwan Corp., 1997.

The contents of this paper reflect the views of the authors and do not necessarily reflect the official views and policies of the FAA.

Publication of this paper sponsored by Committee on Rigid Pavement Design.